Thermodynamic Properties of the $NaNO_3+H_2O$ System

Donald G. Archer[a]

Physical and Chemical Properties Division, National Institute of Standards and Technology, Gaithersburg, Maryland 20899-8381

New equations that describe the thermodynamic properties of the $NaNO_3+H_2O$ system were obtained from previously published measurements for this system. The measured values included in the fitted equations spanned the range of temperatures of approximately 236–425 K for $NaNO_3$(aq) and 16–548 K for $NaNO_3$(cr). New equations and/or values for the following properties are given in the present work: (1) thermal properties of $NaNO_3$(cr) from 0 K to near the lambda transition, 548.6 K, (2) the change in chemical potential for both $NaNO_3$ and H_2O in $NaNO_3$(aq) as a function of temperature, and molality, valid from 236 to 425 K, and the molality range of 0 $mol \cdot kg^{-1}$ to the lesser of the saturation molality or 25 $mol \cdot kg^{-1}$, and (3) standard-state properties for the aqueous solution process. © *2001 by the U.S. Secretary of Commerce on behalf of the United States. All rights reserved.* [S0047-2689(00)00305-6]

Contents

1. Introduction

Nitrates are found in very high concentrations in aqueous phases and also as precipitates in nuclear waste storage tanks throughout the Department of Energy's complex of nuclear-material handling sites. Modeling potential and actual treat-

[a]Electronic mail: donald.archer@nist.gov

ments of these wastes requires various thermodynamic properties, particularly component activities and solubilities. Nitrates are also found in runoff from agricultural activity. When present in drinking water, nitrates may be related to increased risk of a particular type of cancer, i.e., non-Hodgkins lymphoma (96WAR/MAR). As part of our continuing program of providing thermodynamic properties necessary for assessing environmental fates of materials and development of remediation technologies, new equations for the thermodynamic properties of the binary system $NaNO_3+H_2O$ are given here. These equations are valid for conditions relevant to environmental and remediation technologies. The present equations do not extend to the full range of conditions for which $NaNO_3(aq)$ exists. This is because the solubility of $NaNO_3(aq)$ becomes very large, the system becomes miscible near 582.6 K, and the molality-based equations given here are not meaningful for a miscible system.

A second purpose of the present work is to determine the standard-state thermodynamic properties for the solution of sodium nitrate in water. These properties are required for development of a consistent set of standard-state properties for a basis set of substances.

2. Thermodynamic Properties of Sodium Nitrate(cr)

A model for the thermodynamic properties of crystalline sodium nitrate is developed here, valid for temperatures from 0 to $\approx$548 K. Such an equation is required for inclusion of enthalpies of solution as a function of temperature and for the treatment of the phase-equilibria data for $NaNO_3(cr)+NaNO_3(aq)$. A lambda transition for $NaNO_3(cr)$ occurs near 549 K. We have not attempted to model the properties of the solid phase that occurs between the lambda transition near 549 K and the melting temperature near 612 K, as these temperatures are outside the range of accurate data for the aqueous solution and hence outside of the range for which reliable phase equilibria can be calculated.

To obtain thermodynamic properties for the range of temperatures considered here, previous thermodynamic measurements were selected and included in a least-squares representation. All of the selected enthalpy increments and heat capacities were fitted simultaneously by means of a cubic-spline method described previously (92ARC1).

Briefly, the following function, $f(T)$, was used:

$$f(T)=[T\cdot(C^\circ_{p,m}/C^\circ_p)^{-1/3}-bT]/T^\circ, \quad (1)$$

where b was a constant, arbitrarily chosen to be 0.2 for the present case, and where C°_p was 1 $J\cdot K^{-1}\cdot mol^{-1}$ and T° was 1 K. The function $f(T)$ of Eq. (1) was fitted with a cubic spline using polynomials of the form:

$$f(T)=a_i(T-T_i)^3+b_i(T-T_i)^2+c_i(T-T_i)+d_i, \quad (2)$$

where the subscript i referred to the polynomial that contained the specified value of T and spanned the temperature range T_i to T_{i+1}, and a_i, b_i, c_i, and d_i are the coefficients

of the ith polynomial. A particular (T_i, d_i) pair is referred to as a "knot." A "natural spline" end condition (i.e., second derivative equal to 0) was imposed at the highest temperature knot. The end condition imposed at the lowest temperature knot was a value of $-b(-0.2)$ for the first derivative. This was equivalent to assuming that the Debye temperature was independent of temperature near 0 K. (For the purpose of calculation: $T_{i+1}>T>T_i$.) The calculated heat capacity was

$$C^\circ_{p,m}/C^\circ_p=\left(\frac{T}{T^\circ f(T)+bT}\right)^3. \quad (3)$$

Equation (3) was integrated numerically to obtain the enthalpy. The model was fitted to the experimental values with a nonlinear least-squares program. The vector of residuals was calculated using Eq. (3) for the heat capacity or numerical integration of Eq. (3) to obtain enthalpy increments.

Several sets of measurements of the thermal properties of sodium nitrate have been published in the past. Unfortunately, the only measurements for temperatures below 300 K are the early measurements from Southard and Nelson (33SOU/NEL). The measurements from 33SOU/NEL were assigned a square root of variance (srv) of $\pm0.5\%$. The measurements from Sokolov and Schmidt (55SOK/SCH), Janz et al. (64JAN/KEL), and Ichikawa and Matsumoto (83ICH/MAT) were assigned srvs of 1%. All of these measurements were obtained with either adiabatic calorimeters or enthalpy-drop calorimeters. The values reported by Carling (83CAR), Takahashi et al. (88TAK/SAK), and Rogers and Janz (82ROG/JAN) were assigned srvs of 3%; these latter measurements were obtained with differential scanning calorimeters. Reinsborough and Wetmore (67REI/WET) measured enthalpy changes for small changes in temperature. They reported three heat capacity values, and presented the remainder of their values graphically. They tabulated values of $(H_T-H_{T=0\,K})$ that they obtained from graphical integration of their heat capacity values. We calculated enthalpy increments $(H_{T_2}-H_{T_1})$ from the tabulated values where T_1 and T_2 were consecutive temperatures given in the table. These values should be closer to what 67REI/WET actually measured than would be values of $(H_T-H_{T=0\,K})$. These values

TABLE 1. Least-squares estimated knot positions for $NaNO_3(cr)$

T_i (K)	d_i
0	13.8263
20	9.1161
30	8.0902
50	7.2388
100	6.8064
200	7.2934
300	6.1446
400	2.9899
500	-6.1762
538	-19.0485
547	-32.4801
552	-53.0548

TABLE 2. Thermodynamic properties of $NaNO_3(cr)$ calculated from Eqs. (1) and (2)

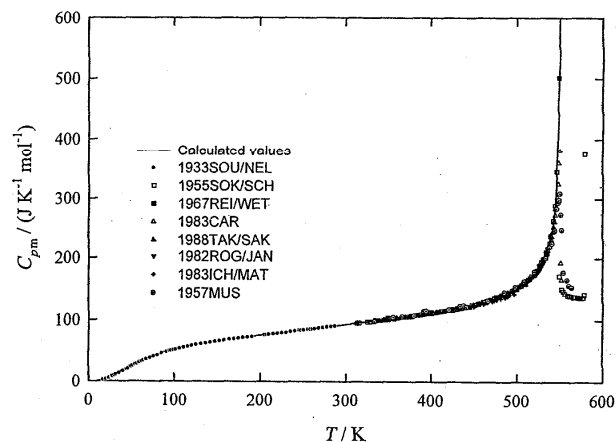| T (K)	$C_{p,m}$ (J·K⁻¹·mol⁻¹)	$H_m(T)-H_m(0\ K)$ (kJ·mol⁻¹)	S_m (J·K⁻¹·mol⁻¹)
5	0.049	0.000	0.016
10	0.417	0.001	0.134
15	1.491	0.005	0.476
20	3.545	0.018	1.163
25	6.384	0.042	2.249
30	9.65	0.082	3.696
35	13.22	0.139	5.449
40	16.95	0.215	7.457
45	20.71	0.309	9.671
50	24.40	0.422	12.045
55	27.98	0.553	14.539
60	31.40	0.701	17.122
65	34.69	0.866	19.764
70	37.68	1.047	22.444
75	40.51	1.243	25.141
80	43.14	1.452	27.840
85	45.58	1.674	30.530
90	47.85	1.907	33.200
95	49.95	2.152	35.844
100	51.91	2.407	38.457
110	55.47	2.944	43.575
120	58.61	3.515	48.539
130	61.40	4.115	53.343
140	63.90	4.742	57.986
150	66.17	5.392	62.473
160	68.26	6.064	66.811
170	70.21	6.757	71.008
180	72.07	7.468	75.074
190	73.87	8.198	79.019
200	75.63	8.946	82.85
220	79.14	10.493	90.23
240	82.65	12.111	97.26
260	86.18	13.799	104.02
280	89.72	15.558	110.53
298.15	92.97	17.216	116.27
300	93.30	17.389	116.84
325	97.8	19.777	124.49
350	102.4	22.280	131.91
375	107.1	24.899	139.13
400	111.9	27.637	146.20
425	117.2	30.500	153.14
450	124.3	33.514	160.03
475	134.8	36.743	167.01
500	151.3	40.305	174.32
520	174.5	43.535	180.65
530	196.4	45.380	184.16
540	234.0	47.513	188.2
545	295.0	48.800	190.5

FIG. 1. Heat capacity of crystalline sodium nitrate against temperature. The line was calculated from the fitted equation. Not all measured values are shown.

positions. The final knot positions are given in Table 1. The number of digits given in Table 1 should be sufficient for calculation of thermodynamic properties and was not meant to be representative of any statistical assessment. Calculated thermodynamic properties of $NaNO_3(cr)$ are given in Table 2.

Figure 1 shows calculated values of the heat capacity of $NaNO_3(cr)$ as a function of temperature. Also shown are values reported in the literature. Near the lambda transition, the differences between the different sets of high temperature measurements become quite large ($\sim 40\%$). In the region of the lambda transition, the values from 83CAR appear to be too small. This could be due to error in the temperature reported by their scanning calorimeter, which may have resulted in the thermogram being shifted to temperatures larger than the true temperature. This shift in temperature is evidenced in the temperature given for the solid–solid phase transition by 83CAR, 550 K, which is approximately 1.5 K larger than that given by most other references. In Fig. 3 of 83ICH/MAT, they showed their own heat capacity results to temperatures very close to the solid–solid transition. However, in their table of ''experimental heat capacities,'' they gave no values between 497.05 K and the temperature of the solid–solid transition (548 K). They gave no acknowledgement of the discrepancy between their table and their figure.

Figure 2 shows the differences of most of the reported values of enthalpy increments or heat capacities from the fitted equation.

A solid–solid transition in $NaNO_3(cr)$ has been reported by 68FER/KJE2 as occurring at 243 K. The bases of this assertion are anomalous changes in electrical resistivity and dielectric constant against temperature in this region. Referring to their interpretation of their results and previous x-ray diffraction results, they concluded that a structural alteration occurred as 243 K, and that ''it is clear that only a minor change in structure is involved, probably other than a geometrical change within the nitrate group.'' 79BAD/KAM re-

were assigned a srv of 1%. The results from Mustajoki (57MUS) and Miekk-Oja (41MIE) were given no weight in the representation.

Representation of the experimental results over the full range of temperature required 12 variable values for the knot
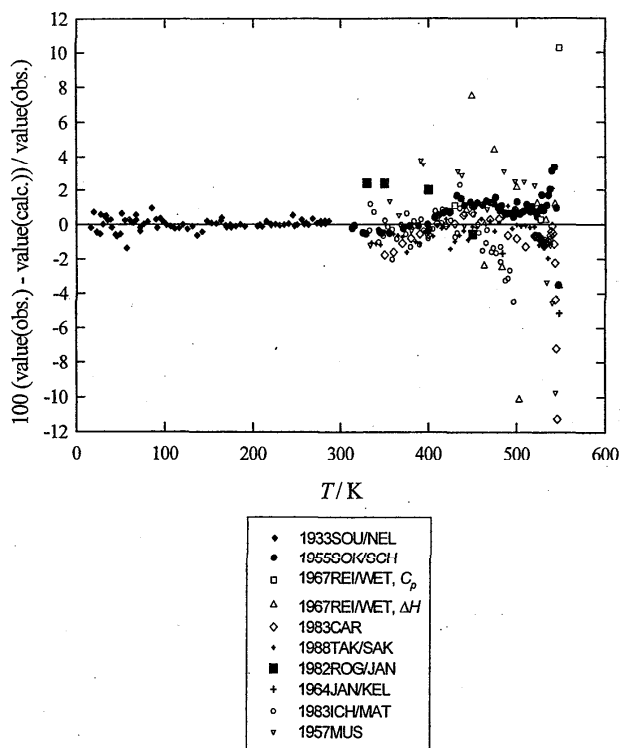
FIG. 2. Comparison of measurements for sodium nitrate to values calculated from the fitted equation.

ported anomalous effects in a differential thermal analysis for NaNO$_3$(cr) in addition to the anomalous effects in the electrical properties. However, no anomaly was apparent in the heat capacity measurements for this temperature range from 33SOU/NEL.

The entropy of NaNO$_3$(cr) at 298 K is determined entirely from the measurements from 33SOU/NEL. If 79BAD/KAM's thermogram is to be believed, then doubt is cast on the entropy obtained from 33SOU/NEL. Because of the contrary reports in the literature, one cannot state a reliable assessment of accuracy for the entropy values given for the crystal. Concomitantly, one cannot assess the accuracy of the entropy of the nitrate ion obtained from measurements on the sodium nitrate system, as well as other nitrate systems for which similar electrical anomalies have been reported (1968 FER/KJE1, 71BJO/FER). It may be noted that 71OWE/KEN examined the heat capacity for two of the nitrates for which low temperature structural changes were reported, RbNO$_3$ and CsNO$_3$, and found no effect in the thermal functions, within their uncertainties. They also found no structural change of CsNO$_3$, at these temperatures, as evidenced by their neutron scattering measurements.

3. Thermodynamic Properties of Sodium Nitrate(aq)

3.1. Treatment of the Thermodynamic Data

The model used here is the Archer extension of Pitzer's ion-interaction equation (91ARC, 73PIT). Because the

model used here is similar to that used previously (1992 ARC2), only a brief description is given here. The fitted equation for the excess Gibbs energy for an arbitrary valence type is

$$\frac{G^E}{n_w RT} = -4IA_\phi \ln(1+bI^{1/2})/b$$
$$+2\nu_M\nu_X(m^2 B_{MX}+m^3 \nu_M z_M C_{MX}), \quad (4)$$

where

$$B_{MX}=\beta_{MX}^{(0)}+2\beta_{MX}^{(1)}[1-(1+\alpha I^{1/2})\exp(-\alpha I^{1/2})]/(\alpha^2 I),$$
$$(4a)$$

and

$$C_{MX}=C_{MX}^{(0)}+4C_{MX}^{(1)}[6-(6+6\alpha_2 I^{1/2}+3\alpha_2^2 I+\alpha_2^3 I^{3/2})$$
$$\times\exp(-\alpha_2 I^{1/2})/]/(\alpha_2^4 I^2), \quad (4b)$$

where $\beta_{MX}^{(0)}$, $\beta_{MX}^{(1)}$, $C_{MX}^{(0)}$ and $C_{MX}^{(1)}$ are adjustable parameters (ion-interaction parameters) that are dependent on temperature and pressure; z_M and z_X (the latter appears later) are the charges of the cation and the anion, respectively; α and b were chosen to be constants with the values 2.0 and 1.2 kg$^{1/2}$·mol$^{-1/2}$, respectively; ν_M and ν_X are the stoichiometric numbers of cations and anions formed upon complete dissociation and n_w is the number of kg of water. A_ϕ is the Debye–Hückel coefficient for the osmotic coefficient. The Debye–Hückel coefficients used in the present work were calculated from the equation of state for water from Hill (90HIL) and the dielectric-constant equation from Archer and Wang (90ARC/WAN). The value of α_2 used in the fitted equation was 2.5 kg$^{1/2}$·mol$^{-1/2}$.

The excess Gibbs energy, G^E, is related to the Gibbs energy of the solution, G, as

$$G^E=G-n_1 G^\circ_{m,1}-n_2 G^\circ_{m,2}+RT\nu n_2\{1-\ln(m/m^\circ)\},$$
$$(5)$$

where n_1 and n_2 are the number of moles of solvent and solute, respectively, m is the stoichiometric molality, ν is the number of ions formed upon complete dissociation of the electrolyte, and m° is 1.0 mol·kg^{-1}. The standard-state molar Gibbs energy for solvent and solute are $G^\circ_{m,1}$ and $G^\circ_{m,2}$, respectively. The standard states were chosen to be pure liquid for the solvent and the hypothetical one molal ideal solution for the solute at the temperature and pressure of interest, rather than at the temperature of interest and an arbitrary pressure.

Appropriate differentiation of Eq. (4) leads to the osmotic coefficient, ϕ, and the stoichiometric activity coefficient, $\gamma_\pm$:

$$\phi - 1 = -|z_M z_X| A_\phi \frac{I^{1/2}}{1 + bI^{1/2}} + m \frac{2\nu_M \nu_X}{\nu} (\beta_{MX}^{(0)} + \beta_{MX}^{(1)}$$

$$\times \exp(-\alpha I^{1/2})) + m^2 \frac{4\nu_M^2 \nu_X z_M}{\nu} (C_{MX}^{(0)} + C_{MX}^{(1)}$$

$$\times \exp(-\alpha_2 I^{1/2})), \tag{6}$$

$$\ln \gamma_\pm = -|z_M z_X| A_\phi \left(\frac{I^{1/2}}{1 + bI^{1/2}} + \frac{2}{b} \ln(1 + bI^{1/2}) \right)$$

$$+ m \frac{2\nu_M \nu_X}{\nu} \left\{ 2\beta_{MX}^{(0)} + \frac{2\beta_{MX}^{(1)}}{\alpha^2 I} \left[1 - \left(1 + \alpha I^{1/2} - \frac{\alpha^2 I}{2} \right) \right. \right.$$

$$\left. \left. \times \exp(-\alpha I^{1/2}) \right] \right\} + m^2 \frac{2\nu_M^2 \nu_X z_M}{\nu} \cdot \{3C_{MX}^{(0)} + 4C_{MX}^{(1)}$$

$$\times [6 - (6 + 6\alpha_2 I^{1/2} + 3\alpha_2^2 I + \alpha_2^3 I^{3/2} - \alpha_2^4 I^2/2)$$

$$\times \exp(-\alpha_2 I^{1/2})]/(\alpha_2^4 I^2)\}. \tag{7}$$

The osmotic coefficient is related to the activity of water, a_w, as: $\phi = -\ln a_w (M_1 \nu m)^{-1}$, where M_1 is the molar mass of the solvent in $\text{kg} \cdot \text{mol}^{-1}$. The relative apparent molar enthalpy, L_ϕ, is

$$L_\phi = \nu |z_M z_X| A_H \ln(1 + bI^{1/2})/2b - 2\nu_M \nu_X RT^2$$

$$\times (mB_{MX}^L + m^2 \nu_M z_M C_{MX}^L), \tag{8}$$

where

$$B_{MX}^L = \left(\frac{\partial \beta_{MX}^{(0)}}{\partial T} \right)_p + 2 \left(\frac{\partial \beta_{MX}^{(1)}}{\partial T} \right)_p [1 - (1 + \alpha I^{1/2})$$

$$\times \exp(-\alpha I^{1/2})]/\alpha^2 I, \tag{9}$$

$$C_{MX}^L = \left(\frac{\partial C_{MX}^{(0)}}{\partial T} \right)_p + 4 \left(\frac{\partial C_{MX}^{(1)}}{\partial T} \right)_p$$

$$\times [6 - (6 + 6\alpha_2 I^{1/2} + 3\alpha_2^2 I + \alpha_2^3 I^{3/2})$$

$$\times \exp(-\alpha_2 I^{1/2})]/(\alpha_2^4 I^2) \tag{10}$$

and where A_H is the Debye–Hückel coefficient for apparent molar enthalpy. The constant-pressure apparent molar heat capacity, $C_{p,\phi}$, is

$$C_{p,\phi} = C°_{p,m,2} + \nu |z_M z_X| A_C \ln(1 + bI^{1/2})/2b$$

$$- 2\nu_M \nu_X RT^2 (mB_{MX}^C + m^2 \nu_M z_M C_{MX}^C), \tag{11}$$

where

$$B_{MX}^C = \left(\frac{\partial^2 \beta_{MX}^{(0)}}{\partial T^2} \right)_p + \frac{2}{T} \left(\frac{\partial \beta_{MX}^{(0)}}{\partial T} \right)_p + 2 \left\{ \left(\frac{\partial^2 \beta_{MX}^{(1)}}{\partial T^2} \right)_p \right.$$

$$\left. + \frac{2}{T} \left(\frac{\partial \beta_{MX}^{(1)}}{\partial T} \right)_p \right\} [1 - (1 + \alpha I^{1/2}) \exp(-\alpha I^{1/2})]/\alpha^2 I, \tag{12}$$

$$C_{MX}^C = \left(\frac{\partial^2 C_{MX}^{(0)}}{\partial T^2} \right)_p + \frac{2}{T} \left(\frac{\partial C_{MX}^{(0)}}{\partial T} \right)_p$$

$$+ 4 \left\{ \left(\frac{\partial^2 C_{MX}^{(1)}}{\partial T^2} \right)_p + \frac{2}{T} \left(\frac{\partial C_{MX}^{(1)}}{\partial T} \right)_p \right\}$$

$$\times [6 - (6 + 6\alpha_2 I^{1/2} + 3\alpha_2^2 I + \alpha_2^3 I^{3/2})$$

$$\times \exp(-\alpha_2 I^{1/2})]/(\alpha_2^4 I^2) \tag{13}$$

and where A_C is the Debye–Hückel coefficient for apparent molar heat capacity and $C°_{p,m,2}$ is the standard-state molar heat capacity of the solute. A reference molality was used in the fitting equations to avoid representation of the extreme temperature dependence of the usual ideal-solution standard state. In these terms, the apparent molar heat capacity is

$$C_{p,\phi} + c_{p,w}^* / n_r = C_p(m_r)/n_r + \nu |z_M z_X| A_C \ln\{(1 + bI^{1/2})/$$

$$(1 + bI_r^{1/2})\}/2b - 2\nu_M \nu_X RT^2 \{(mB_{MX}^C(m)$$

$$- m_r B_{MX}^C(m_r) + \nu_M z_M [m^2 C_{MX}^C(m)$$

$$- m_r^2 C_{MX}^C(m_r)]\}, \tag{14}$$

where $C_p(m_r)$ is the heat capacity of a quantity of solution containing 1 kg of solvent at the desired temperature and pressure and $c_{p,w}^*$ is the heat capacity of 1 kg of water.

The partial molar Gibbs energy of the solute in its standard state at temperature T and pressure p, $G°_{m,2,T,p}$, may be written in terms of the above equations as

$$G°_{m,2,T,p} = G°_{m,2,T_r,p_r} + \frac{n_1 G°_{m,1,T_r,p_r} - n_1 G°_{m,1,T,p}}{n_r}$$

$$+ \frac{G_{T_r,p_r,m_r}^E - G_{T,p,m_r}^E}{n_r} - (T - T_r)$$

$$\times \left(S°_{2,m,T_r,p_r} + \frac{n_1 S°_{1,m,T_r,p_r}}{n_r} + \frac{S_{T_r,p_r,m_r}^E}{n_r} \right)$$

$$- T \int_{T_r}^T \frac{1}{T^2} \int_{T_r}^T \{C_{p,p_r}(m_r)/n_r\} dT' \, dT'', \tag{15}$$

where

$$S_{T_r,p_r}^E = -\left(\frac{\partial G_{T_r,p_r}^E}{\partial T} \right)_p \tag{16}$$

The equation that describes the solubility of the anhydrous solid phase is

$$\Delta_{sol} G°_m = G°_{m,2} - G°_{m,cr} = -2RT \ln(m_s \gamma_{\pm,s}/m°), \tag{17}$$

where $G°_{m,2}$ and $G°_{m,cr}$ are the molar Gibbs energies for the solute and the anhydrous crystal phase at a given T and p, respectively. $\Delta_{sol} G°_m$ is the standard-state molar Gibbs energy for the solution process of the anhydrous crystal phase and m_s and $\gamma_{\pm,s}$ are the saturation molality and the mean

stoichiometric activity coefficient for the solute at saturation, respectively. Of course, $G°_{m,2}$ and $G°_{m,cr}$ cannot be evaluated and so Eq. (17) was rewritten as

$$\Delta_{sol}G°_T = \Delta_{sol}G°_{T_r} + \{G°_{m,2,T} - G°_{m,2,T_r}\}$$

$$- \{G°_{m,cr,T} - G°_{m,cr,T_r}\}$$

$$= -2RT \ln(m_s\gamma_{\pm,s}/m°). \tag{18}$$

The first term in curly braces in Eq. (18) was obtained from Eq. (15), the second term in curly braces in Eq. (18) was obtained from the equations for $NaNO_3$(cr) given previously.

Solubility measurements were included in the global data fit. The Gibbs energy of solution at the reference temperature, T_r, and reference pressure, p_r, was treated as an adjustable parameter, as was $S°_{2,m,T_r,p_r}$. In addition, the experimental solubility results make some contribution to the determination of the parameters for the excess Gibbs energy for the solution through Eq. (18).

The literature sources for the measurement database are given in Table 3. Table 3 contains each reference, the relevant temperature and molality ranges, the number of observations of each data type, and an estimate of the uncertainty of the literature data. Also given are the root-mean-square and average deviations of the equation from the data set.

The ion-interaction parameters for the excess Gibbs energy for the $NaNO_3$(aq) solution were expressed as

$$\beta^{(0)}_{MX} = f(1/T)/m°, \tag{19}$$

$$\beta^{(1)}_{MX} = f(2,T)/m°, \tag{20}$$

$$C^{(0)}_{MX} = f(3,T)/m°^2, \tag{21}$$

$$C^{(1)}_{MX} = f(4,T)/m°^2, \tag{22}$$

where

$$f(i,T) = [b_{i,1} + b_{i,2}T/(1000\,K) + b_{i,3}\{T/(500\,K)\}^2$$

$$+ b_{i,4}T°/(T - 215\,K) + b_{i,5}1 \times 10^4\{T°/(T$$

$$- 215\,K)\}^3 + b_{i,6}100\{T°/(T - 215\,K)\}^2$$

$$+ b_{i,7}200(T°/T)^2 + b_{i,8}\{T/(500\,K)\}^3 \tag{23}$$

and where $T°$ is 1.0 K. $C_p(m_r)/n_r$ was taken to be a function of T as

$$C_{p,p_r}(m_r)/n_r = [b_{6,1} + b_{6,2}T/(300\,K)]C°_p, \tag{24}$$

where $C°_p$ is 1.0 kJ·K^{-1}·mol^{-1}. The least-squares estimated parameters, $b_{i,j}$, are given in Table 4. The absence of a value for a particular $b_{i,j}$ from Table 4 indicates that it was not used in the final least-squares procedure. In the ion-interaction model, the temperature dependence of the viral coefficients is given as an arbitrary linear function that is assumed to converge to the true behavior. In such a representation, one adds and subtracts large quantities to arrive at a final small quantity. This necessarily requires large numbers of digits. The number of required digits is increased further because we wish to accurately obtain several higher temperature de-

rivatives. There may be a few too many digits for the parameters given in Table 4, but it is not clear where to truncate these numbers, in fact, truncation would depend on which property is to be calculated. We believe that it is better to give a few too many digits than too few, for obvious reasons. Tables 5–7 give values of various parameters and thermodynamic functions against which to test calculations.

3.2. Agreement with the Experimental Results for Sodium Nitrate(aq)

3.2.1. Activity Results

Osmotic coefficients were calculated from measured differences in vapor pressure between the solution and the solvent as

$$\phi = \frac{(G°_{m,1} - G°_{m,1,g})}{RTvmM_1}, \tag{25}$$

where the difference in chemical potential for the liquid and the vapor at the temperature and pressure of the solution, $G°_{m,1} - G°_{m,1,g}$, was calculated from the equation of state for water. Osmotic coefficients were also calculated from measured differences of the freezing temperatures of water in a sodium nitrate solution from that of pure water by means of the equation given by 75CRA/VAN. Osmotic coefficients were determined from measured isopiestic ratios by means of the reference equation for NaCl(aq) given in 92ARC2 or the reference equation for KCl(aq) given in 99ARC, as the case may be.

Figure 3 shows differences of the osmotic coefficients for $NaNO_3$(aq), obtained from measured properties of the solvent in the solution, from the present fitted equation for temperatures near 300 K. Osmotic coefficients from isopiestic molality determinations, 35ROB, 64KIR/LUK, 65KIR/LUK, were all in good agreement with the fitted equation, as were the freezing point measurements from 32SCA/PRE. At low molalities, <1 mol·kg^{-1}, there was a small biasing of the osmotic coefficients from 32SCA/PRE from those of 35ROB. Similar biasing from these two sources was also observed for NaBr(aq) (95KAR/ARC). The osmotic coefficients calculated from the vapor pressure measurements described by 62KAN/GRO ($m \geq 2$ mol·kg^{-1}) agreed very well with osmotic coefficients calculated from the isopiestic molalities reported in 65KIR/LUK, i.e., worse case difference ≈ 0.0015.

Also shown in Fig. 3 are differences of Wu and Hamer's equation (80WU/HAM) for the osmotic coefficient from the present equation. For molalities >6 mol·kg^{-1}, their equation showed a systematic bias relative to the present equation, and also relative to the measurements reported by both 65KIR/LUK and 62KAN/GRO. 80WU/HAM did not consider the measurements from either 64KIR/LUK or 65KIR/LUK. The osmotic coefficient values that 80WU/HAM tabulated as resulting from their calculation using the vapor pressure measurements from 62KAN/GRO differed from those calculated here. Their values (80WU/HAM) were 0.003 larger than ours for $m = 10$ mol·kg^{-1}; 0.005 larger for

TABLE 3. Literature sources for the activity and thermal properties of $NaNO_3(aq)$

Reference	Temperature range (K)	Molality range (mol·kg^{-1})	n^a	Type	σ_{est}^{b}	σ_{fit}^{c}	δ_{fit}^{d}
35ROB	298.15	0.1–6.0	49	ϕ	0.003	0.0031	−0.0005
64KIR/LUK	298.15	3.1–6.0	6	ϕ	0.003	0.0021	−0.0019
65KIR/LUK	298.15	0.9–9.9	40(2)	ϕ	0.003	0.0032	−0.0009
49STO/ROB	298.15	m_{sat}	1	ϕ	0.005	0.008	0.008
90VOI/DIT	373.45	1.0 16.0	8(1)	ϕ	0.01	0.0064	−0.0015
62KAN/GRO	293.15–298.15	1.0–10	19	p_s-p_w	0.01^e	0.0036	0.0008
37PEA/HOP	298.15	0.1–10.8	18	p_s-p_w	0.02^e	0.018	0.014
67SHP/MIS	274.15	0.3–8	19	p_s-p_w	0.03, $m_L=2^e$	0.047	−0.0096
67SHP/MIS	298.15	0.3–10.8	24	p_s-p_w	0.03, m_L-2^e	0.016	−0.0083
67SHP/MIS	323.15	0.3–14	27	p_s-p_w	0.03, $m_L=2^e$	0.019	−0.0050
67SHP/MIS	348.15	0.3–17	30	p_s-p_w	0.03, $m_L=2^e$	0.019	−0.009
93BOS/RIC	424.96	1.5–23	8	p_s-p_w	0.02, $m_L=15^e$	0.099	−0.008
81EGO/ZAR	423.15	1.0–24	11	p_s-p_w	U	0.044	0.032^e
32SCA/PRE	T_{fus}	0.0008–1.7	33	$\Delta_{fus}T$	^{f}	0.0046	0.0017
68HOL	T_{fus}	2.2–7.19	5	$\Delta_{fus}T$	^{g}	0.0071	−0.0034
40SHP	T_{fus}	3.6–7.3	3	$\Delta_{fus}T$	^{h}	0.035	0.024
18ROD	T_{fus}	2.4–7.3	6	$\Delta_{fus}T$	^{h}	0.010	−0.009
70VIL/IRI	T_{fus}	1.5–3.0	8	$\Delta_{fus}T$	^{i}	0.024	0.018
58HAR/SHR	298.15	5×10^{-4}–0.02	7	$\gamma_{\pm}$	0.002	0.0037	−0.0011
96MAR/KHO	298.15	0.1–3.5	15	$\gamma_{\pm}$	U	0.023	−0.0070
77RAB/TUM	298.15	0.001–3.3	12	$\gamma_{\pm}$	U	0.0060	0.0005
22EDG/SWA	293–303	m_{sat}	11	p_{sat}	^{j}	0.019	−0.016
29ADA/MER	283–313	m_{sat}	6	p_{sat}	^{j}	0.032	−0.014
37DIE	289.4–298.4	m_{sat}	6	p_{sat}	^{j}	0.016	0.010
73SHE/RUC	375.45–392.15	m_{sat}	2	p_{sat}	^{k}	0.0060	0.002^l
49CAR/HAR	303–363	m_{sat}	7	p_{sat}	U	0.073	−0.055^l
98APE, 93APE	277.6–310.3	m_{sat}	31	p_{sat}	U	0.113	0.035^l
1883THO	298.15	0.19–7.4	4(1)	ΔL_ϕ	0.1	0.11	−0.047^m
08BIS	298.15	0.19–7.4	6	ΔL_ϕ	U	0.23	−0.20^m
14STA	291.15	0.19–7.4	19	ΔL_ϕ	0.1	0.10	0.041^m
18PRA	288.15–298.15	0.14–2.2	12	ΔL_ϕ	0.05	0.052	0.005^m
21RIC/ROW	293.15	0.14–2.2	4	ΔL_ϕ	0.03	0.026	−0.012^m
28NAU	291.16	0.002–0.3	7	ΔL_ϕ	0.025	0.019	0.001^m
30LAN/ROB	298.15	2×10^{-4}–0.1	26	ΔL_ϕ	0.01	0.0088	0.0052^m
67GRE/SNE	298.15	0.03–2	2	ΔL_ϕ	0.08	0.051	0.049^m
25MON	289.15	0.5–9.4	8	$\Delta_{sol}H_m$	U	3.5	−3.5^m
70KHR/AKH	291.15, 298.15	8.5–12.5	17	$\Delta_{sol}H_m$	0.6	0.49	−0.46^m
67MIS/SHP	298.15	0.05–10.2	20	$\Delta_{sol}H_m$	0.3	0.21	−0.13^m
89PAL/BAR	298.15	0.001	1	$\Delta_{sol}H_m$	0.3	0.5	0.5^m
46VOS/PON	298.15	0.18	1	$\Delta_{sol}H_m$	0.3	−0.04	−0.04^m
90PEK/VAC	298.15	0.007–0.026	5	$\Delta_{sol}H_m$	0.3	0.27	0.27^m
59VAN/WEN	298.15	0.28	1	$\Delta_{sol}H_m$	0.2	0.6	0.6^m
67KRE/EGO	298.15	?	1	$\Delta_{sol}H_m$	0.3	0.075	0.075^m
37LAN/MAR	298.15	0.12	1	$\Delta_{sol}H_m$	0.3	0.24	0.24^m
12HAI	294.15	0.14	1	$\Delta_{sol}H_m$	0.3	0.14	−0.14^m
90PEK/VAC	298.15	0.5–10.4	39	$\Delta_{sol}H_m$	0.3	0.18	0.048^n
67MIS/SHP	274.15	0.01–7.0	11	$\Delta_{sol}H_m$	U	0.60	0.54^m
67MIS/SHP	323.15	0.02–13	17	$\Delta_{sol}H_m$	U	0.68	−0.65^m
21RIC/ROW	293.15	2.2	1	$c_{p,s}/c_{p,w}$	0.002	0.0034	0.0034^o
29RAN/ROS	298.15	0.05–2.5	11	$c_{p,s}/c_{p,w}$	0.008	0.0065	−0.0050^p
38?DA	298.15	2.6	1	$c_{p,s}$	U	0.012	−0.012^q
67EPI/STA	298.15	1–6	9	$c_{p,s}$	0.004	0.0033	0.0019^r
73PEM/PUC	298.15	0.5–1.0	2	$c_{p,s}$	0.004	0.0048	−0.0029^q
73PUC/MAT	298.15	0.6–10.9	6(1)	$c_{p,s}$	0.021	0.0039	−0.0011^q
73PUC/MAT	323.15	0.6 10.9	6	$c_{p,s}$	0.021	0.003	0.0018^q
73PUC/MAT	348.15	0.6–10.9	6	$c_{p,s}$	0.052	0.052	0.0030^q
73PUC/MAT	373.15	0.6–10.9	6	$c_{p,s}$	0.10	0.017	−0.005^q
73PUC/MAT	423.15	0.6–10.9	6	$c_{p,s}$	0.10	0.080	−0.044^q
77ENE/SIN	298.15	0.05–0.17	6	$c_{p,\phi}$	0.004	0.0026	0.0023^r
78ROU/MUS	298.15	0.03–2.1	34	$c_{p,\phi}$	0.004	0.0026	0.0018^r
2000CAR/ARC	236–285	0.1–10.0	142	$c_{p,s}-c_{p,w}$	^{s}	0.067	0.0014

TABLE 3. Literature sources for the activity and thermal properties of $NaNO_3(aq)$—Continued

Reference	Temperature range (K)	Molality range (mol·kg⁻¹)	n^a	Type	σ_{est}^b	σ_{fit}^c	δ_{fit}^d
04BER	273–392	m_s	8	m_s	0.025	0.005	-0.002^t
15REI	278–373	m_s	4	m_s	0.05	0.0099	0.0085^t
29CHR	262.6–393.3	m_s	19	m_s	0.02	0.007	-0.0001^t
29COR/KRO	273–373	m_s	7(1)	m_s	0.05	0.013	-0.0008^t
31KRA	367.2–388.05	m_s	3	m_s	0.1	0.010	0.010^t
37BEN/GJE	375.2–416.2	m_s	2	m_s	0.5	0.047	0.037^t
40SHP	255.6–303.15	m_s	7	m_s	0.2	0.094	0.039^t
57MAK/KAM	298.15	m_s	1	m_s	0.1	0.008	0.008^t
63ZHR/SHE	283.15–303.15	m_s	3	m_s	0.1	0.0070	0.0067^t
68HOL	255.7–333.15	m_s	10	m_s	0.05	0.016	-0.0076^t
70YAK/ZAL	298.15	m_s	1	m_s	0.05	0.008	0.008^t
70PLE/BOB	293.15–298.15	m_s	2	m_s	0.05	0.006	0.006^t
73SHE/RUC	375–392	m_s	2	m_s	0.05	0.0079	-0.0067^t
80KOL/ZHI	323.15–348.15	m_s	2	m_s	0.1	0.030	0.029^t
85SAD/SBI	298.15	m_o	1	m_o	0.05	0.024	0.024^t
96KOR/SOI	293.15–333.15	m_s	4(1)	m_s	0.05	0.013	0.006^t

$^a n$ is the number of observations; a number in parentheses indicates the number of observations rejected from the data set.

$^b \sigma_{est}$ is an estimated square root of variance used for weighting the measurements. The letter U indicates that these points were given an insignificant weight in the least-squares procedure. In the cases where a value is given for m_L, the expected square root of the variance is taken to be the first of the two given values for $m > m_L$ and taken to be the first value multiplied by (m_L/m) for $m < m_L$.

$^c \sigma_{fit}$ is the rms deviation of the measurements from the model.

$^d \delta_{fit}$ is the average deviation of the measurements from the model.

^{e}Values of $\sigma_{est}, \sigma_{fit}, \delta_{fit}$ are given in terms of the osmotic coefficient.

^{f}Values of σ_{est} were calculated as the uncertainty in osmotic coefficient due to an uncertainty of 0.001 K or 0.003, whichever was larger. σ_{fit} and δ_{fit} given in terms of osmotic coefficient.

^{g}Values of σ_{est} were calculated as the uncertainty in osmotic coefficient due to an uncertainty of 0.1 K. σ_{fit} and δ_{fit} given in terms of osmotic coefficient.

^{h}Values of σ_{est} were calculated as the uncertainty in osmotic coefficient due to an uncertainty of 0.2 K. σ_{fit} and δ_{fit} given in terms of osmotic coefficient.

^{i}Values of σ_{est} were calculated as the uncertainty in osmotic coefficient due to an uncertainty of 0.5 K. σ_{fit} and δ_{fit} given in terms of osmotic coefficient.

^{j}Values of σ_{est} were calculated as the uncertainty in osmotic coefficient due to an uncertainty of 0.03 $\times 10^{-3}$ MPa. σ_{fit} and δ_{fit} given in terms of osmotic coefficient.

^{k}Values of σ_{est} were calculated as the uncertainty in osmotic coefficient due to an uncertainty of 5 $\times 10^{-4}$ MPa. σ_{fit} and δ_{fit} given in terms of osmotic coefficient.

$^l \sigma_{fit}$ and δ_{fit} given in terms of osmotic coefficient.

^{m}Values of $\sigma_{est}, \sigma_{fit}, \delta_{fit}$ are given in kJ·mol⁻¹.

^{n}Type is differential enthalpy of solution. Values of $\sigma_{est}, \sigma_{fit}, \delta_{fit}$ are given in kJ·mol⁻¹.

$^o \sigma_{est}$ was calculated on the basis of 0.002 of $c_{p,s}/c_{p,w}$. σ_{fit} and δ_{fit} are given in terms of $C_{p,\phi}$ and have units of kJ·K⁻¹·mol⁻¹.

$^p \sigma_{est}$ was 0.008 kJ·K⁻¹·mol⁻¹ in $C_{p,\phi}$. σ_{fit} and δ_{fit} are given in terms of $C_{p,\phi}$ and have units of kJ·K⁻¹·mol⁻¹.

$^q \sigma_{est}$ was calculated on the basis of the tabulated value $c_{p,s}$ in J·K⁻¹·g⁻¹. σ_{fit} and δ_{fit} are given in terms of $C_{p,\phi}$ and have units of kJ·K⁻¹·mol⁻¹.

$^r \sigma_{est}$ was 0.004 kJ·K⁻¹·mol⁻¹ in $C_{p,\phi}$. σ_{fit} and δ_{fit} are given in terms of $C_{p,\phi}$ and have units of kJ·K⁻¹·mol⁻¹.

$^s \sigma_{est}$ was taken to be the values from 2000CAR/ARC, which varied with concentration and temperature. σ_{fit} and δ_{fit} are given in terms of $C_{p,\phi}$ and have units of kJ·K⁻¹·mol⁻¹.

$^t \sigma_{est}$ was calculated on the basis of the tabulated value for solubility in mol·kg⁻¹. σ_{fit} and δ_{fit} are given in terms of Gibbs energy of solution and have units of kJ·mol⁻¹.

$m = 3$ mol·kg⁻¹; and 0.011 larger for $m = 1$ mol·kg⁻¹. The systematic bias of their equation from the present work arose primarily from this discrepancy in calculated values of ϕ from vapor pressure measurements. The good agreement of the ϕ values we calculated here from the 62KAN/GRO measurements with values of ϕ obtained from isopiestic molality determinations confirms that the present treatment of 62KAN/GRO is more accurate than that of 80WU/HAM.

There are some reports in the literature of the use of specific-ion electrodes to determine $\gamma_\pm$ for $NaNO_3(aq)$. Although specific-ion electrodes do not give true thermodynamic properties, differences of $\gamma_\pm$ from the fitted equation are shown in Fig. 3 for two of these reports, for completeness. The values given by 96MAR/KHO and 77RAB/TUM showed rms errors of 0.023 and 0.006 from the fitted equation, respectively.

TABLE 4. Least-squares estimated parameters for the model of thermodynamic properties of $NaNO_3(aq)$.[a]

Parameter	Value	Parameter	Value	Parameter	Value
$b_{1,1}$	$-0.740\,945\,476\,063\,445$	$b_{2,1}$	$0.942\,480\,517\,141\,718$	$b_{3,1}$	$-1.256\,894\,249\,139\,012E-002$
$b_{1,2}$	$5.301\,436\,224\,607\,53$	$b_{2,2}$	$-1.269\,733\,285\,173\,06$	$b_{3,2}$	
$b_{1,3}$	$-3.051\,861\,561\,954\,69$	$b_{2,3}$		$b_{3,3}$	$2.565\,842\,333\,766\,710E-002$
$b_{1,4}$		$b_{2,4}$	$-29.342\,131\,357\,890\,1$	$b_{3,4}$	$-4.337\,541\,064\,223\,505E-002$
$b_{1,5}$	$-9.695\,523\,827\,708\,996E-003$	$b_{2,5}$		$b_{3,5}$	$3.885\,940\,284\,279\,465E-004$
$b_{1,6}$	$7.228\,823\,686\,725\,505E-002$	$b_{2,6}$		$b_{3,6}$	
$b_{1,7}$		$b_{2,7}$		$b_{3,7}$	$3.249\,053\,927\,944\,20$
$b_{1,8}$	$1.164\,522\,357\,292\,16$	$b_{2,8}$		$b_{3,8}$	$-1.577\,851\,899\,506\,610E-002$
$b_{4,1}$	$0.131\,128\,066\,446\,870$	$b_{6,1}$	$0.546\,919\,291\,455\,574$	$\Delta_{sol}G°m,T_r$	$-6.218\,6\pm0.020\,kJ\cdot mol^{-1}$
$b_{4,2}$		$b_{6,2}$	$-2.102\,117\,445\,539\,875E-002$	$S°_{m,2,T_r}$	$204.92\pm0.25\,J\cdot K^{-1}\cdot mol^{-1}$
$b_{4,3}$					
$b_{4,4}$	$-21.196\,903\,086\,982\,7$				
$b_{4,5}$					
$b_{4,6}$	$1.402\,192\,362\,469\,12$				
$b_{4,7}$					
$b_{4,8}$	$0.604\,277\,271\,768\,524$				

[a]The $\pm$ values are 95% confidence intervals within the global data representation. The listed uncertainty for $S°_{m,2,T_r}$ does not include the uncertainty in $S°_{m,cr,T_r}$, see text.

Vapor pressure measurements for temperatures removed from ambient have been reported in the literature (67SHP/MIS, 70PUC/MAT, 93BOS/RIC). These measurements were adequately represented by the equation. Figure 4 shows the agreement of the equation with vapor pressure measurements at 423.15 K (70PUC/MAT) and 424.96 K (93BOS/RIC). Figure 4 also shows extrapolated values of vapor pressure calculated from the equation at 452.78 K compared with values reported by 93BOS/RIC. Agreement of the fitted equation with osmotic coefficients calculated from the isopiestic molality determinations for 373.45 K given by 90VOI/DIT was considered acceptable, particularly when one considers the uncertainty of the osmotic coefficient of $CaCl_2(aq)$ at this temperature (see e.g., 95RAR/ARC).

There have been reported many determinations of the vapor pressure of water over solute-saturated solutions of $NaNO_3(aq)$. Most of these studies did not report determination of the saturation molality. Therefore, in order to include and/or examine these determinations, the saturation molality was calculated from the present equations. Figure 5 shows values of the osmotic coefficient for the saturation molality against temperature from several of these studies. Measurements from 22EDG/SWA, with the exception of one value; 29ADA/MER; 37DIE; 49STO/ROB; all agreed with the fitted equation within their claimed uncertainties. More recent

measurements of the saturation vapor pressure have been reported by Apelblat (93APE, 98APE). The only discussion of measurement uncertainty given in those two references was a claim of "sensitivity" of 0.003 kPa. This "sensitivity" corresponds to an uncertainty in the osmotic coefficient of ±0.016 at 278 K and ±0.003 at 299 K. Differences of osmotic coefficients obtained from Apelblat's vapor pressures from values calculated from the fitted equation are shown in Fig. 5, where curves have been drawn through these residuals so as to aid the eye. The pattern of systematic error for 93APE is clearly much larger than that calculated from the claimed "sensitivity." The absolute value of the systematic bias is about 20 times the sensitivity at the lowest temperatures and about 50 times the value at the highest temperature. Additionally, the systematic bias of the 93APE measurements was similar to that observed previously for $NaBr(aq)$ (95RAR/ARC) and reinforces the suggestion made there that the systematic bias resulted from artifacts in the experimental method and would thus be common to all the measurements thereby produced. The 98APE measurements also showed a temperature-dependent systematic bias. This bias was particularly pronounced at low temperatures, where the error appears to be more than 20 times greater than 1998APE's sensitivity.

TABLE 5. Calculated values of A_ϕ, $\beta_{MX}^{(0)}$, $\beta_{MX}^{(1)}$, $C_{MX}^{(0)}$, and $C_{MX}^{(1)}$

T (K)	A_ϕ (kg$^{1/2}\cdot$mol$^{-1/2}$)	$\beta_{MX}^{(0)}$ (kg$\cdot$mol^{-1})	$\beta_{MX}^{(1)}$ (kg$\cdot$mol^{-1})	$10^3 C_{MX}^{(0)}$ (kg$^2\cdot$mol^{-2})	$10^3 C_{MX}^{(1)}$ (kg$^2\cdot$mol^{-2})
273.15	0.376 422	$-0.012\,158\,8$	0.091 059 0	0.499 291	$-0.093\,404\,3$
298.15	0.391 476	0.002 304 99	0.211 028	0.004 126 0	0.024 609 1
323.15	0.410 277	0.012 357 9	0.260 857	$-0.286\,222$	0.110 253
348.15	0.433 068	0.018 601 7	0.280 054	$-0.418\,555$	0.183 839
373.15	0.459 887	0.021 821 6	0.283 146	$-0.443\,139$	0.253 879

TABLE 6. Calculation values of $G°_{m,2}-G°_{m,2,T_r}$, $H°_{m,2}-H°_{m,2,T_r}$, $S°_{m,2}-S°_{m,2,T_r}$, and $C°_{p,\phi}$

T (K)	$G°_{m,2}-G°_{m,2,T_r}$ (kJ·mol⁻¹)	$H°_{m,2}-H°_{m,2,T_r}$ (kJ·mol⁻¹)	$S°_{m,2}-S°_{m,2,T_r}$ (J·K⁻¹·mol⁻¹)	$C°_{p,\phi}$ (J·K⁻¹·mol⁻¹)
273.15	5.186	1.843	6.519	−136.4
298.15	0.000	0.000	0.00	−35.4
323.15	−5.097	−0.545	−1.767	−14.4
348.15	−10.163	−0.890	−2.794	−15.0
373.15	−15.202	−1.343	−4.049	−21.8

3.2.2. Enthalpy and Heat Capacity Results

Measurements of enthalpies of dilution for NaNO₃(aq) date mostly from before 1935. Almost all of the previously reported measurements are for initial molalities that were smaller than 2.5 mol·kg⁻¹ and all were for temperatures less than 300 K. These measurements were all represented within the estimated uncertainties given in Table 3 and for those that could be so compared, these uncertainties were in accord with previous examinations (e.g., 99ARC). Differences of the reported enthalpies of dilution from values calculated from the present equation are shown in Fig. 6.

There are two sets of measurements of the enthalpy of solution against a wide range of concentration at 298.15 K (76MIS/SHP, 90PEK/VAC). The former source reported enthalpies of solution of NaNO₃(cr) into water and the latter reported enthalpies of solution of NaNO₃(cr) into water and into NaNO₃(aq). 90PEK/VAC referred to the latter quantity as a "differential" enthalpy of solution. However, their measurements were only an approximation to the true differential enthalpy of solution. Rather, the dissolution of NaNO₃(cr) into NaNO₃(m_i) to form a solution of composition NaNO₃(m_f) is expressed as

$$\Delta_{sol}H_m = \Delta_{sol}H°_m + m_fL_\phi(m_f) - m_iL_\phi(m_i). \quad (26)$$

These particular measurements from 90PEK/VAC were incorporated into the least-squares solution using Eq. (26). Figure 7 shows values of both the integral and the true differential enthalpies of solution calculated from the fitted equation for 298.15 K. Also shown in Fig. 7 are measured values of the integral enthalpy of solution and the approximate values of the differential enthalpy of solution from 90PEK/VAC. Values given by 82WAG/EVA are also shown in Fig. 6. Their values are larger than the enthalpy of solution measurements from 70KHR/AKH, 76MIS/SHP, and the differential enthalpy of solution values from 90PEK/VAC, throughout most of the concentration region.

There are new measurements of the heat capacity of NaNO₃(aq) for temperatures ranging from 285 to 236 K, or less, and for compositions of 0.1 to 10 mol·kg⁻¹ (2000CAR/ ARC). There are also new measurements of the heat capacity of water for temperatures less than 270 K (2000ARC/CAR) that we believe to be more accurate than the values upon which are based equations of state for water. Therefore, incorporation of the new low-temperature heat capacity measurements for NaNO₃(aq) was not as straightforward as it may seem. The heat capacity of water from 2000ARC/CAR was significantly smaller than that calculated from recent previous equations of state at the lowest measured temperatures. If one incorporates the specific heat capacity of NaNO₃(aq), $c_{p,s}$, in the fitted data set, then the apparent molar heat capacity, which is calculated through combination of $c_{p,s}$ with $c_{p,w}$ from Hill's equation of state (90HIL), becomes much too negative as temperature decreases. This is because the heat capacity of water calculated from Hill's equation is much larger than values at the lower temperatures of the present measurements. It is beyond the scope of the present article to present a new equation of state for water
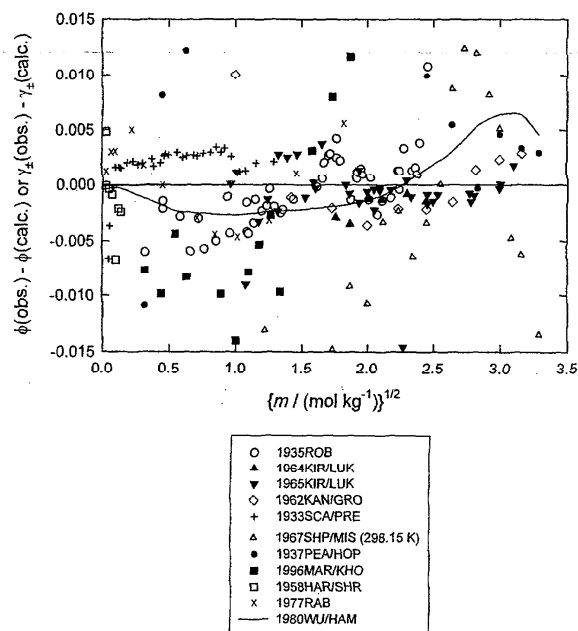
TABLE 7. Calculation values of the osmotic coefficient, ϕ

T (K)	m (mol·kg⁻¹)					
	0.1	0.5	1.0	2.0	5.0	10.0
273.15	0.9165	0.8907	0.8147	0.7713	0.7234	0.7248
298.15	0.9219	0.8792	0.8570	0.8301	0.7907	0.7713
323.15	0.9220	0.9220	0.8787	0.8638	0.8339	0.8085
348.15	0.9191	0.8932	0.8890	0.8827	0.8595	0.8353
373.15	0.9141	0.8909	0.8919	0.8916	0.8713	0.8501

O	1935ROB
▲	1964KIR/LUK
▼	1965KIR/LUK
◇	1962KAN/GRO
+	1933SCA/PRE
△	1967SHP/MIS (298.15 K)
●	1937PEA/HOP
■	1996MAR/KHO
□	1958HAR/SHR
x	1977RAB
—	1980WU/HAM

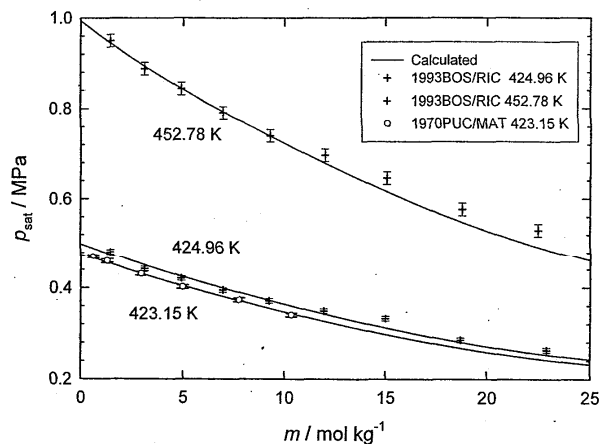FIG. 3. Differences of measured osmotic coefficients from the model for near ambient temperatures.

FIG. 4. Vapor pressure of NaNO₃(aq) at elevated temperatures. The solid lines were calculated from the least-squares estimated model. The line shown for 452.78 K is an extrapolation of the model.

FIG. 6. Differences of measured enthalpies of dilution from the model for temperatures near 298.15 K.

that is more accurate for supercooled solutions. Alternately, one could incorporate $C_{p,\phi}$ calculated from the present heat capacity values for water and NaNO₃(aq). Although this would be better, it is troubled by the fact that one is using

conflicting values of the heat capacity of water in the calculations. We opted to incorporate the quantity $(c_{p,s}-c_{p,w})$ into the fitted data set. From there, the program calculated $C_{p,\phi}$ using the equation of Hill for water and fitted these
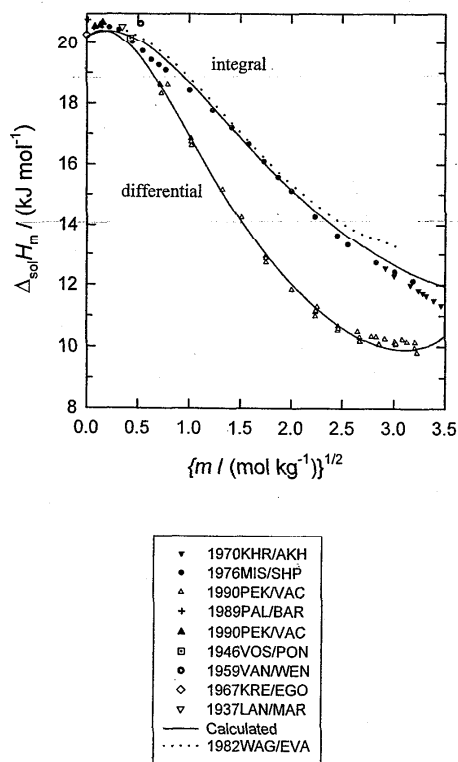

FIG. 5. Values of the osmotic coefficient for saturated solutions of NaNO₃(aq) against temperature. The solid curve was calculated from the least-squares estimated model. The two broken curves are representations of the residuals calculated for 93APE and 98APE, drawn so as to show the trend of bias with respect to temperature.

FIG. 7. Enthalpies of solution of NaNO₃(aq) calculated from the least-squares model and measured values. The upper solid curve is the integral enthalpy of solution. The lower solid curve is the differential enthalpy of solution. The dotted curve was obtained from 82WAG/EVA.
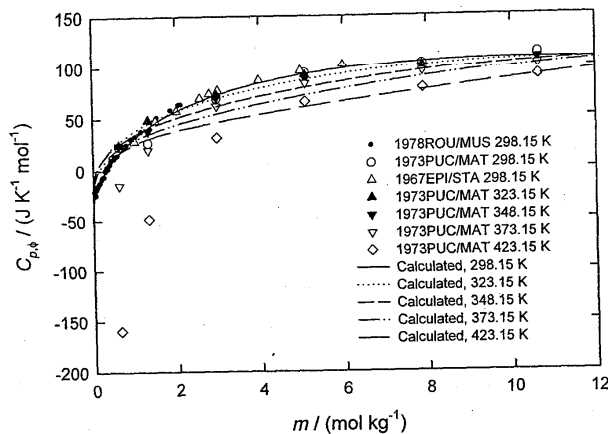
FIG. 8. Heat capacity of NaNO₃(aq) from 298.15 to 423.15 K against molality. The lines were calculated from the least-squares model.

FIG. 9. Heat capacity of NaNO₃(aq) from 236 to 280 K against square root of molality. The lines were calculated from the least-squares model. The symbols represent some of the measured values given in 2000CAR/ARC.

$C_{p,\phi}$ values, as well as all the other values in the database. The values of $C_{p,\phi}$ calculated in this way are not the same as those given in Table 3 of 2000CAR/ARC. The values in 2000CAR/ARC's Table 3 are more accurate because they are based on the most accurate properties of water that are available, we believe. From the fitting parameters and the above-mentioned equations, one may recover an approximate value of the heat capacity of the solution by calculating $c_{p,s}$ from $C_{p,\phi}$ and $c_{p,w}$ from Hill et al., take the difference of these two values and then add the heat capacity of water obtained from Table 3 of 2000ARC/CAR.

The new equation represented most of the new heat capacity values, calculated as discussed previously, $(c_{p,s} - c_{p,w})$, to within experimental uncertainties. However, there are some notable discrepancies. Misrepresentation of $c_{p,s}$ for (6–10) mol·kg⁻¹ NaNO₃(aq) becomes large as $T \to 236$ K. This is because $C_{p,p_r}(m_r)/n_r$ is expected to be a slowly varying function of T, even to temperatures below 236 K (see measured values in 2000CAR/ARC). Equation (14) indicates that $C_{p,\phi}$ calculated from the present equations contains the quantity $C_{p,p_r}(m_r)/n_r - c_{p,w}^*/n_r$, where $c_{p,w}^*$ is calculated from the equation of state of water. But the heat capacity of water calculated from the equation of state was about 8% larger than the values determined in 2000ARC/CAR. This difference in calculated property for water from the true property results in some misrepresentations of the fitted $(c_{p,s} - c_{p,w})$ at the lowest temperatures for the solutions, particularly for 6–10 mol·kg⁻¹ NaNO₃(aq). These misrepresentations could be reduced by adding to Eq. (24) terms of the sort $b_{6,j} f\{(T - y)^{-x}; x > 0; y \sim (210 - 230 \text{ K})\}$. However, such terms cause the divergence of the calculated specific heat capacity of 10 mol·kg⁻¹ NaNO₃(aq). as $T \to y$; a behavior that is contrary to the observed behavior. That one must adapt Eq. (24) to give unreal behavior of $c_{p,s}$ for 10 mol·kg⁻¹ NaNO₃(aq). as $T \to y$ in order to obtain reasonable representations of the $c_{p,s}$ for $236 \text{ K} \leq T < 250 \text{ K}$ (i.e., $T > y$) supports the conclusion that the values of c_p for water given by 2000ARC/CAR are more accurate than the earlier values
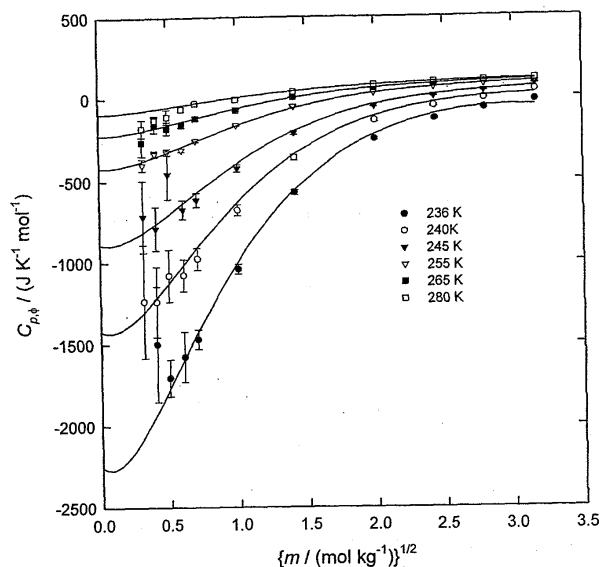
reported in the literature and upon which the equation of state for water was based empirically. To a certain extent, the ion-interaction parameters corrected for some of the inaccuracies in the calculated properties of water. However, this means that at these low temperatures the ion-interaction parameters represented something different than they otherwise would have, had more accurate properties of water been obtained from established equations of state for water. The limiting factor in the quality of representation of the supercooled properties of NaNO₃(aq), specifically, and other electrolyte solutions, generally, appears to be the accuracy of established equations of state for water for temperatures below 270 K.

Representation of heat capacities over the range of temperatures considered here is shown in Figs. 8 and 9. There was some misrepresentation of the 423 K heat capacities from 73PUC/MAT at the lowest concentrations, this is partially a result of the unusual behavior of the osmotic coefficient measurements at the higher temperatures and perhaps also partially due to the extended range of concentration included in the representation at the elevated temperatures.

4. Phase Equilibria, Thermodynamic Properties of the Solution Process, and the Ion-interaction Parameters

Measurements of the anhydrous solubility and the ice freezing points of the NaNO₃+H₂O system are shown in Fig. 10 for the temperature range of 250 to near 400 K. The equations presented here predicted that the invariant equilibrium NaNO₃(aq)+NaNO₃(cr)+H₂O(cr)+H₂O(g) exists at 255.81 K, 7.144 mol·kg⁻¹, and 0.13 kPa. These values are in
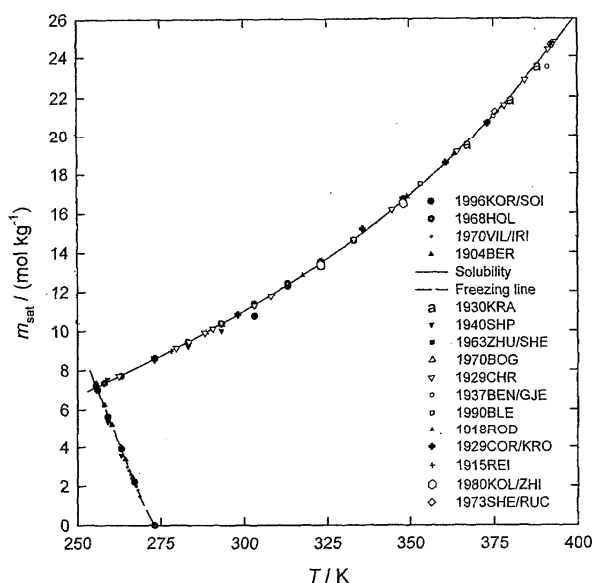
Fig. 10. Values of the solubility of the anhydrous solute and the ice-freezing line calculated from the model compared to measured values.

TABLE 8. Calculated values of the saturation molality and the vapor pressure of the saturated solution.

T/K	m_{sat}/mol·kg^{-1}	p_{sat}/kPa
273.15	8.584	0.4894
278.15	9.014	0.6879
283.15	9.454	0.9531
288.15	9.903	1.3029
293.15	10.365	1.7584
298.15	10.839	2.3445
303.15	11.327	3.0902
308.15	11.831	4.0288
313.15	12.352	5.1981
318.15	12.892	6.6408
323.15	13.453	8.4043
328.15	14.036	10.541
333.15	14.644	13.108
338.15	15.280	16.168
343.15	15.944	19.788
348.15	16.641	24.037
353.15	17.372	28.991
358.15	18.141	34.728
363.15	18.950	41.323
368.15	19.803	48.880
373.15	20.701	57.465

reasonable agreement with, but slightly different from, the values 255.69 K and 7.35 mol·kg^{-1} (18ROD); 255.05 K and 7.233 mol·kg^{-1} (26NIK); 255.65 K and 7.33 mol·kg^{-1} (40SHP); and 255.7 K and 7.19 mol·kg^{-1} (68HOL). The small differences can be ascribed to the required thermodynamic consistency required within the present model and the uncertainties of the solubility and temperature measurements themselves.

The calculated values of the ice freezing temperatures are in good agreement with the values reported by 32SCA/PRE and 68HOL. The agreement is less good with the measurements from 18ROD, 40SHP, and 70VIL/IRI. The values from these references showed average systematic biases from the fitted equation of −0.2, +0.34, and +0.2 K, respectively.

From the present equations one may calculate the vapor pressure of water over a saturated solution. Such values might still have usefulness in humidity control at specific temperatures. Values of the saturation vapor pressure calculated from the present equation are given in Table 8.

The standard-state properties for the solution process at T_r=298.15 K and p_r=0.1 MPa were calculated to be $\Delta_{sol}G°_m = (-6.219 \pm 0.022)$ kJ·mol^{-1} and $\Delta_{sol}S°_m = (88.654 \pm 0.25)$ J·K^{-1}·mol^{-1}, where the $\pm$ values are 95% confidence intervals within the least-squares solution. (The uncertainty in Table 4 associated with the parameter $S°_{m,2,T_r}$ is not truly the uncertainty in that quantity, rather it is the uncertainty in the standard-state molar entropy of solution.) By difference, the standard-state enthalpy of solution can be calculated to be, $\Delta_{sol}H°_m = 20.213$ kJ·mol^{-1}. These values can be compared to values given by 82WAG/EVA,

$\Delta_{sol}G°_m = -6.15$ kJ·mol^{-1} and $\Delta_{sol}S°_m = 88.9$ J·K^{-1}·mol^{-1}. The difference of their value for the Gibbs energy of solution from that calculated here is about three times our 95% confidence interval.

We cannot compare the present values with values from the CODATA Key Values for Thermodynamics (89COX/WAG) for the following reasons. In the method used to present thermodynamic properties in 89COX/WAG, the enthalpies of formation and the entropies of Na⁺(aq) and NO₃⁻(aq) were tabulated as "key" values. The entropy of NO₃⁻(aq), according to Note 44 and Annex II of 89COX/WAG, was obtained from a least-squares calculation involving many reactions, including several reactions that involved nitrate compounds, primarily enthalpies of solution and Gibbs energies of solution. Enthalpy of solution and Gibbs energy of solution values for NaNO₃ were indicated as having been included in that list of reactions. However, 89COX/WAG did not describe, in any fashion, the residuals for their least-squares calculation, nor did they tabulate, or in any other way make available, all of their least-squares-calculated parameters. In the case of NaNO₃, the undisclosed parameters are the optimized values for the entropy and enthalpy of formation of NaNO₃(cr). Without these concealed properties, which are arguably just as "key" as the entropy of NO₃⁻(aq), because the latter was calculated in conjunction with the former, one cannot calculate any of the thermodynamic properties for the solution of NaNO₃ into water that would be consistent with the CODATA Key Values. One also cannot combine the values tabulated by 89COX/WAG with values from other thermodynamic compendia because
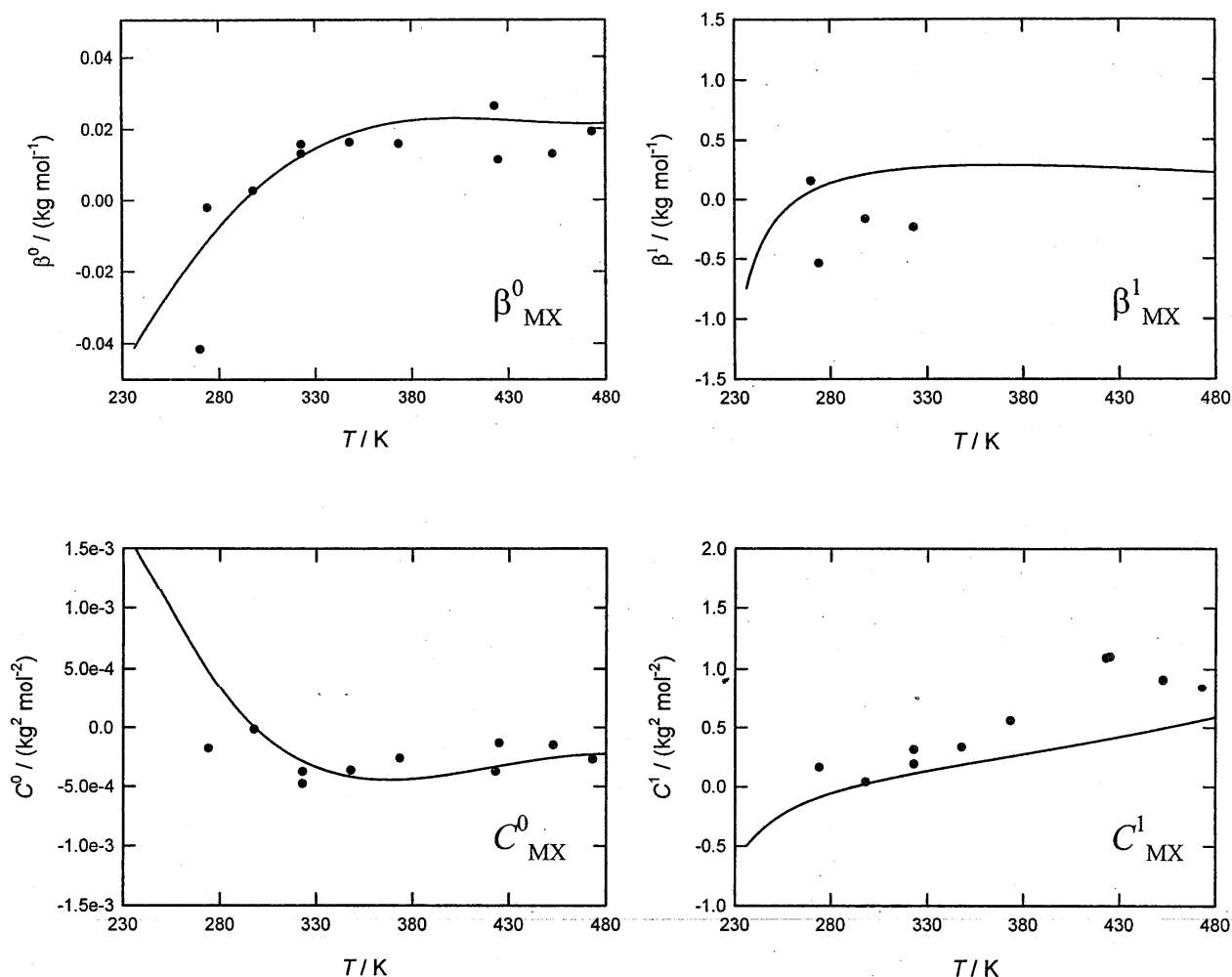
FIG. 11. Values of the ion-interaction parameters against temperature. Lines are calculated from the global representation and are extrapolations for T >426 K. The symbols were obtained from isothermal fits of activity data

they have different basis sets. This is a general problem with the CODATA Key Values and can be summarized as follows. Many of the values are part of a least-squares solution and are not useful without the additional, but undisclosed, properties that were simultaneously optimized in that least-squares calculation. And they cannot be used in conjunction with other thermodynamic compendia because even the most basic information for so doing was not included in the 89COX/WAG document.

We show in Fig. 11, as lines, the ion-interaction parameters calculated from the least-squares solution. Above 430 K, the calculated values are extrapolations. Also shown are values obtained from isothermal fitting of activity measurements. (Above 330 K, $\beta_{MX}^{(1)}$ was not included in the isothermal fitting, but it did have a presence in the global fitting. This may be the source of differences of the globally obtained $C_{MX}^{(1)}$ from the values obtained from isothermal fitting.) Of particular interest is the behavior of $\beta_{MX}^{(0)}$ at low temperatures. In the Pitzer formalism, this parameter is re-

lated to second virial coefficient, loosely derived from McMillan–Mayer considerations. In this context, when ion association beyond that of Poisson–Boltzmann electrostatic attraction becomes strong enough to affect properties at low concentrations, $\beta_{MX}^{(0)}$ should become negative. This is what one sees with aqueous sodium nitrate. At 298.15 K, estimates of the association constant are that it is small, e.g., 72RID/LOC, from spectroscopic data and assignment of values of species activity coefficients, estimated that the association constant for ion-pair formation was only 0.06 at 298.15 K. The osmotic coefficients that one calculates for the lowest concentrations for which 32SCA/PRE measured freezing-point depressions are consistent with the Debye–Hückel function used in the present work. From the freezing point determinations, osmotic coefficient values smaller than the Debye–Hückel function do not occur until m >0.7 mol·kg^{-1}. This is consistent with ion association that is not strong enough to require explicit incorporation of ion association in the model.

5. References

1883THO Thomsen, J., *Thermochemische Untersuchungen* (Barth, Leipzig, 1883).

04BER Berkeley, E., Philos. Trans. R. Soc. London, Ser. A **203**, 189 (1904).

08BIS Bishop, F. L., Phys. Rev. **26**, 169 (1908).

12HAI Haigh, F. L., J. Am. Chem. Soc. **34**, 1137 (1912).

14STA Stahlberg, A., Ofvers Finska Vetens. Soc. Forh. **57**, 1 (1914).

15REI Reinders, W., Z. Anorg. Chem. **93**, 202 (1915).

18PRA Pratt, F. R., J. Franklin Inst. **185**, 663 (1918).

18ROD Rodebush, W. H., J. Am. Chem. Soc. **40**, 1204 (1918).

21RIC/ROW Richards, T. W. and Rowe, A. W., J. Am. Chem. Soc. **43**, 770 (1921).

22EDG/SWA Edgar, G. and Swan, W. O., J. Am. Chem. Soc. **44**, 570 (1922).

25MON Mondain-Monval, P., Compt. Rend. **3**, 72 (1925).

26NIK Nikolajew, W. M., J. Russ. Phys. Chem. Soc. **58**, 557 (1926), quoted in Linke, W. F., *Solubilities, Inorganic and Metal-organic Compounds*, 4th ed. (American Chemical Society, Washington, DC, 1965).

28NAU Naude, S. M., Z. Phys. Chem. **135**, 209 (1928).

29ADA/MER Adams, J. R. and Merz, A. R., Ind. Eng. Chem. **21**, 305 (1929).

29CHR Chretien, A., Ann. Chim. (Paris) **12**, 9 (1929).

29COR/KRO Cornec, E. and Krombach, H., Ann. Chim. **12**, 215 (1929).

29RAN/ROS Randall, M. and Rossini, F. D., J. Am. Chem. Soc. **51**, 322 (1929).

30LAN/ROB Lange, E. and Robinson, A. L., Z. Phys. Chem. Abt. A **148**, 97 (1930).

31KRA Kracek, F. C., J. Am. Chem. Soc. **53**, 2609 (1931).

32SCA/PRE Scatchard, G., Prentiss, S. S., and Jones, P. T., J. Am. Chem. Soc. **54**, 2690 (1932).

33SOU/NEL Southard, J. C. and Nelson, R. A., J. Am. Chem. Soc. **55**, 4865 (1933).

35ROB Robinson, R. A., J. Am. Chem. Soc. **57**, 1165 (1935).

37BEN/GJE Benrath, A., Gjedebo, F., Schiffers, B., and Wunderlich, H., Z. Anorg. Chem. **231**, 285 (1937).

37DIE Diesnis, M., Ann. Chim. **7**, 5 (1937).

37LAN/MAR Lange, E. and Martin, U., Z. Phys. Chem. Abt. A **180**, 233 (1937).

37PEA/HOP Pearce, J. N. and Hopson, H., J. Phys. Chem. **41**, 535 (1937).

38ZDA Zdanovskii, A. B., Zh. Fiz. Khim. **12**, 106 (1938).

40SHP Shpunt, S. J., Zh. Prikl. Khim. (St. Petersburg) **13**, 19 (1940).

41MIE Miekk-Oja, H. A., Ann. Acad. Sci. Fenn. Ser. AI: Math. No. 7, 1 (1941).

46VOS/PON Voskresenskaya, N. K. and Ponomareva, K. S., J. Phys. Chem. USSR **20**, 433 (1946).

49CAR/HAR Carr, D. S. and Harris, B. L., Ind. Eng. Chem. **41**, 2014 (1949).

49STO/ROB Stokes, R. H. and Robinson, R. A., Ind. Eng. Chem. **41**, 2013 (1949).

55SOK/SCH Sokolov, V. A. and Schmidt, N. E., Izv. Sekt. fiz.-khim. Analiza Inst. Obshchei Neorg. Khim. **26**, 123 (1955).

57MAK/KAM Makin, A. V. and Kamaukhov, A. S., Russ. J. Inorg. Chem. **2**, 331 (1957).

57MUS Mustajoki, A., Ann. Acad. Sci. Fenn., Ser. AI. Math. No. 6, 1 (1957).

58HAR/SHR Harned, H. S. and Shropshire, J. A., J. Am. Chem. Soc. **80**, 2618 (1958).

59VAN/WEN Van Tassel, J. H. and Wendlandt, W. W., J. Am. Chem. Soc. **81**, 813 (1959).

62KAN/GRO Kangro, W. and Groeneveld, A., Z. Phys. Chem. **32**, 110 (1962).

63ZHR/SHE Zhravlev, E. F., Sheveleva, A. D., Bogdanovskaya, R. L., Kudryashov, S. E., and Shchurov, V. A., Zh. Neorg. Khim. **8**, 1955 (1963).

64JAN/KEL Janz, G. J., Kelly, F. J., and Perano, J. L., J. Chem. Eng. Data **9**, 133 (1964).

64KIR/LUK Kirgintsev, A. N. and Luk'yanov, A. V., Russ. J. Phys. Chem. **38**, 867 (1964).

65KIR/LUK Kirgintsev, A. N. and Luk'yanov, A. V., Russ. J. Phys. Chem. **38**, 653 (1965); **38**, 389 (1965).

67EPI/STA Epikhin, Yu. A. and Stakhanova, M. S., Zh. Fiz. Khim. **41**, 2148 (1967).

67GRE/SNE Greyson, J. and Snell, H., J. Chem. Eng. Data **16**, 73 (1967).

67KRE/EGO Krestov, G. A. and Egorova, I. V., Theor. Exp. Chem. **3**, 71 (1967).

67MIS/SHP Mishchenko, K. P. and Shpigel, L. P., Zh. Obshch. Khim. **37**, 2145 (1967).

67REI/WET Reinsborough, V. C. and Wetmore, F. E. W., Aust. J. Chem. **20**, 1 (1967).

67SHP/MIS Shpigel', L. P. and Mishchenko, K. P., Zh. Pirkl Khim. (S. Petersberg) **40**, 680 (1967).

68FER/KJE1 Fermor, J. H. and Kjekshus, A. Acta Chem. Scand. **22**, 836 (1968).

68FER/KJE2 Fermor, J. H. and Kjekshus, A., Acta Chem. Scand. **22**, 1628 (1968).

68HOL Homberg, K. E., *Phase Diagrams of Some Sodium and Potassium Salts in Light and Heavy Water* (Aktiebolaget Atomenergi, Stockholm, Sweden, 1968).

70KHR/AKH Khrenova, T. L., Akhumov, E. I., and Ahulika, L. P., Zh. Prikl. Khim. (St. Petersburg) **43**, 1599 (1970).

70PLE/BOB Plekhotkin, V. F. and Bobrovskaya, L. P., Russ. J. Inorg. Chem. **15**, 842 (1970).

70PUC/MAT Puchkov, L. V. and Matashkin, V. G., Zh. Prikl. Khim. (S.-Petersburg) **43**, 1963 (1970).

70VIL/IRI Vilcu, R. and Irinei, F., Bull. Soc. Chim. Belg. **79**, 3 (1970).

70YAK/ZAL Yakimov, M. A., Zalkind, E. V., and Vlasova, E. P., Russ, J. Inorg. Chem. **15**, 103 (1970).

71BJO/FER Bjorseth, O., Fermor, J. H., and Kjekshus, A., Acta Chem. Scand. **25**, 3791 (1971).

71OWE/KEN Owen, W. R. and Kennard, C. H. L., Aust. J. Chem. **24**, 1295 (1971).

72RID/LOC Riddell, J. D., Lockwood, D. J., and Irish, D. E., Can. J. Chem. **50**, 2951 (1972).

73PEM/PUC Pemrov, G. I. and Puchkov, L. V., Zh. Prikl. Khim. (St. Petersburg) **46**, 2233 (1973).

73PIT Pitzer, K. S., J. Phys. Chem. **77**, 268 (1973).

73PUC/MAT Puchkov, L. V., Matveeva, R. P., and Baranova, T. L., Zh. Prikl. Khim. (St. Petersburg) **46**, 443 (1973).

73SHE/RUC Shenkin, Ya. S., Ruchnova, S. A., and Rodionova, N. A., Russ. J. Inorg. Chem. **18**, 123 (1973).

75CRA/VAN Craft, Q. D. and VanHook, W. A., J. Solution Chem. **4**, 923 (1975).

77ENE/SIN Enea, O., Singh, P. P., Woolley, E. M., McCurdy, K. G., and Hepler, L. G., J. Chem. Thermodyn. **9**, 731 (1977).

77RAB/TUM Rabinovich, V. A. and Tumob, B. E., Elektrokhimiya **13**, 306 (1977).

78ROU/MUS Roux, A., Musbally, G. M., Perron, G., Desnoyers, J. E., Singh, P. P., Woolley, E. M., and Hepler, L. G., Can. J. Chem. **5**, 24 (1978).

79BAD/KAM Badr, Y. A. and Kamel, R., Phys. Status Solidi A **53**, K161 (1979).

80WU/HAM Wu, Y. C. and Hamer, W. J., J. Phys. Chem. Ref. Data **9**, 513 (1980).

80KOL/ZHI Kol'ba, V. I., Zhikharaev, M. I., and Sukhanova, L. P., Russ. J. Inorg. Chem. **25**, 1583 (1980).

81EGO/ZAR Egorov, V. Ya., Zarembo, V. I., Soboleva, N. G., and Puchkov, L. V., J. Appl. Chem. USSR **54**, 1031 (1981).

82ROG/JAN Rogers, D. J. and Janz, G. J., J. Chem. Eng. Data **27**, 424 (1982).

82WAG/EVA Wagman, D. W., Evans, W. H., Parker, V. B., Schumm, R. H., Halow, I., Bailey, S. M., Churney, K. L., and Nuttall, R. L., J. Phys. Chem. Ref. Data **11**, Suppl. 2 (1982).

83CAR Carling, R. W., Thermochim. Acta **60**, 265 (1983).

83ICH/MAT Ichikawa, K. and Matsumoto, T., Bull. Chem. Soc. Jpn. **56**, 2093 (1983).

85SAD/SBI Sadokhina, L. A., Sbitneva, V. N., and Zimina, G. V., Russ. J. Inorg. Chem. **30**, 1084 (1985).

88TAK/SAK Takahashi, Y., Sakamoto, R., and Kamimoto, M., Int. J. Thermophys. **9**, 1081 (1988).

89COX/WAG Cox, J. D., Wagman, D. D., and Medvedev, V. A., *CODATA Key Values for Thermodynamics* (Hemisphere, Washington, DC, 1989).

89PAL/BAR Palecz, B., Barczynska, J., and Taniewska-Osinska, S., Thermochim. Acta **150**, 121 (1989).

90ARC/WAN Archer, D. G. and Wang, P., J. Phys. Chem. Ref. Data **19**, 371 (1990).

90HIL Hill, P. G., J. Phys. Chem. Ref. Data **19**, 1233 (1990).

90PEK/VAC Pekarek, V., Vacek, V., and Kolarik, S., J Sol. Chem. **19**, 555 (1990).

90VOI/DIT Voigt, W., Dittrich, A., Haugsdal, B., and Grjotheim, K., Acta Chem. Scand. **44**, 12 (1990).

91ARC Archer, D. G., J. Phys. Chem. Ref. Data **20**, 509 (1991).

92ARC1 Archer, D. G., J. Phys. Chem. Ref. Data **21**, 1 (1992).

92ARC2 Archer, D. G., J. Phys. Chem. Ref. Data **21**, 793 (1992).

93APE Apelblat, A. E., J. Chem. Thermodyn. **25**, 63 (1993).

93BOS/RIC Bossmann, E., Richter, J., and Stark, A., Ber. Bunsenges. Phys. Chem. **97**, 240 (1993).

95RAR/ARC Rard, J. A. and Archer, D. G., J. Chem. Eng. Data **40**, 170 (1995).

96KOR/SOI Korin, E. and Soifer, L., J. Chem. Eng. Data **41**, 885 (1996).

96MAR/KHO Marcos-Arroyo, M., Khoshkbarchi, M. K., and Vera, J. H., J. Sol. Chem. **25**, 983 (1996).

96WAR/MAR Ward, M. H., Mark, S. D., Cantor, K. P., Weisenburger, D. D., Correa-Villasenor, A., and Zahm, S. H., Epidemiology **7**, 465 (1996).

98APE Apelblat, A. E., J. Chem. Thermodyn. **30**, 59 (1998).

99ARC Archer, D. G., J. Phys. Chem. Ref. Data **28**, 1 (1999).

2000ARC/CAR Archer, D. G. and Carter, R. W., J. Phys. Chem. B **104**, 8563 (2000).

2000CAR/ARC Carter, R. W. and Archer, D. G., Phys. Chem. Chem. Phys. **2**, 5138 (2000).